Cross sections for electron scattering from furan molecules: Measurements and calculations

Czesław Szmytkowski,* Paweł Możejko, Elżbieta Ptasińska-Denga, and Agnieszka Sabisz
Atomic Physics Group, Faculty of Applied Physics and Mathematics, Gdańsk University of Technology, ulica G. Narutowicza 11/12, 80-233 Gdańsk, Poland
(Received 10 May 2010; published 8 September 2010)

Electron-scattering cross sections have been determined for the furan (C_4H_4O) molecule, both experimentally and theoretically. An absolute total cross section (TCS) has been measured over energies from 0.6 to 400 eV using a linear electron-transmission method. The TCS energy function is dominated with a very broad enhancement, between 1.2 and 9 eV; on the low-energy side, some resonant structures are visible. Integral elastic (ECS) and ionization (ICS) cross sections have been also calculated up to 4 keV in the additivity rule approximation and the binary-encounter-Bethe approach, respectively. Their sum, ECS + ICS, is in a very good agreement with the measured TCS above 70 eV.

DOI: 10.1103/PhysRevA.82.032701 PACS number(s): 34.80.Bm, 34.80.Gs

I. INTRODUCTION

The observation that slow electrons produced by primary ionizing radiation can induce strand breaks in the DNA [1] stimulated an increasing interest in experimental and theoretical studies concerning electron interactions with molecules of biological importance, their constituents, and/or analogs. Among subunits of diverse biocompounds are heterocycle molecules or their derivatives. The simplest five-membered heterocycle molecule with an oxygen atom in the ring is furan (Fig. 1). It may serve as a prototype of a furanose-form building unit of biomolecules. Thus, investigations of electron-induced reactions with furan are useful for understanding and modeling electron-assisted processes in living cells. Furthermore, furan is known to be formed during thermal food processing and, as a possible human carcinogen, is in the field of interest of the nutrition industry [2,3]. Also, due to its release into the atmosphere, it is of interest to the environmental sciences [4].

Furan has been noticed and studied for years but there are, to date, few experimental studies of electron interactions with its gaseous phase. Early works were concerned with the electron-impact excitation of low electronic levels [5–8] or the inner shells [9] of the furan molecule. Some attention has been devoted also to the formation of the negative-ion temporary states (resonances) in the electron-furan scattering: in particular, two shape resonant states centered near 1.7 and 3.1 eV have been noticed in the low-energy electron-transmission experiments [5,10]; a broad resonance around 6 eV has been found [11] in the excitation function of the C–H stretch vibrations; and various fragment anions observed between 3 and 13 eV in the dissociative electron attachment experiments [12,13] have also a resonant origin. Theoretical works [14,15] reveal the resonant features in the elastic and electronically inelastic electron scattering from furan at low impact energy. However, all the aforementioned electron-scattering experiments present the intensities in relative units only, which makes it difficult to speculate on the contributions of specific processes to scattering dynamics. Very recently, dissociation and fragmentation processes that produce electronically excited atomic and molecular fragments have been studied in furan [16] using the electron-impact optical excitation technique. Finally, high-energy electron diffraction [17,18] has been employed to determine the molecular structure of furan.

Recently, we have carried out a series of investigations concerning the electron scattering from heterocyclic organic compounds [19–21], and furan stands as a continuation of our previous studies. In this paper, we report on the measurements of the absolute electron-scattering total cross section (TCS) for furan, from 0.6 to 400 eV, and on calculations of the integrated elastic and ionization cross sections at intermediate and high energies.

II. MEASUREMENTS

The electron-scattering total cross sections (TCSs) reported in this paper have been measured by employing the linear electron-transmission (ET) technique. In the ET method the TCS is related to the transparency of the target of a pressure p for an electron beam of given energy E based on the Bouguer–de Beer–Lambert (BBL) relationship,

$$\sigma_T(E) = \frac{k\sqrt{T_t T_m}}{p\,L} \ln \frac{I_0(E)}{I_p(E)},$$

where $I_0(E)$ and $I_p(E)$ are the intensities of the electron beam transmitted through the reaction cell in the absence and presence of the target, respectively. The pressure p of the target is measured in the center of the cell with the absolute mks capacitance manometer. Since the temperature of the manometer sensor, $T_m = 322$ K, is higher by a few degrees than the temperature of the target cell, T_t, a correction of pressure readings due to the thermal transpiration effect [22] has been necessary. The L is the length of the electron pathway within the target—assumed equal to the geometrical distance (=30.5 mm) between the entrance and exit cell apertures; k is the Boltzmann constant.

The electron spectrometer used for the TCS measurements consists of an electron-beam source (an electron gun coupled to a 127° electrostatic cylindrical monochromator and an array of electron lenses) followed with a reaction chamber and an electron detecting unit [a retarding-field (rf) set of lenses and a Faraday cup (FC)]. The spectrometer electron optics is housed

*czsz@mif.pg.gda.pl

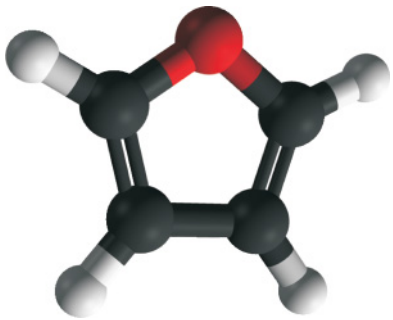

FIG. 1. (Color online) Schematic of the furan molecule, C_4H_4O, geometry.

in a vacuum chamber with the background pressure lower than 40 μPa.

The collimated electron beam of required energy E, with an energy spread $\Delta E \leqslant 0.1$ eV [full width at half maximum (FWHM)], is injected into the reaction cell filled with sample vapor at room temperature. The electrons leaving the scattering volume through the exit aperture are energy-discriminated by the rf analyzer and eventually are collected by the FC detector. The acceptance angle of the used electron detector system, defined by the lens apertures, is 0.7 msr. To ensure that trajectories of the unscattered electrons are straight lines within the reaction and the FC collector volumes, an intensity of the ambient magnetic field in the electron optics region is kept below 0.1 μT. The details of the setup and data processing have been described elsewhere [23].

The sample of furan, obtained from Sigma Aldrich, was of a stated purity better than 99.9%. Prior to use, the sample was subjected to several liquid-nitrogen freeze-pump-thaw cycles to remove volatile impurities. The whole sample-handling system has been maintained at a constant temperature of 299 K in order to prevent pressure fluctuations in the target line; the boiling point of furan is about 5 K higher.

Measurements at a given electron-impact energy were carried out in 5–14 series typically consisting of 6–10 individual runs. It was established that the cross sections obtained in different series at the same energy were independent, within the limits of statistical uncertainties, of the applied incident electron current (0.1–100 pA). Independence of the measured TCS on the target pressure (0.1–0.24 Pa) has been also proved. The final value of the experimental TCS at each particular energy (presented in Table I and Fig. 2) is the weighted mean of the averages from different series of single runs. The statistical uncertainty of the TCS results (one standard deviation of the weighted mean value) is usually well below 1%, excluding the lowest and highest energies employed (i.e., below 1.5 eV and above 150 eV, where the random uncertainties increase to almost 2%).

It is important to identify factors which may systematically distort the particular quantities (see the BBL formula) measured in the present experiment and used to determine the TCS value. There are two effects which are everpresent in the electron-transmission experiments and can influence the TCS measurements. The first one is associated with the unavoidable effusion of the target particles through the scattering cell orifices. A presence of the target particles in the electron optics volume, especially in the electron gun region, can substantially influence the intensity of the primary electron beam. To keep the conditions in the electron optics volume invariable throughout the experiment, irrespective of whether the target is present or absent in the reaction cell, the target vapor is dosed alternately into the cell or into the cell environment, so that the residual target pressure in the electron optics region is practically constant, below 0.2 mPa. The target particles effusing into surrounding of the scattering cell orifices change also the effective path length on which electrons may interact with molecules as well as the target density along the electron

TABLE I. Absolute total cross sections (TCS) measured for electron impact on furan molecules, C_4H_4O, in units of 10^{-20} m^2.

Energy (eV)	TCS	Energy (eV)	TCS	Energy (eV)	TCS	Energy (eV)	TCS
0.6	26.0	3.0	48.4	9.1	49.8	60	32.5
0.7	27.2	3.1	48.6	9.6	49.2	70	31.2
0.8	28.3	3.2	48.4	10.1	48.9	80	29.6
0.9	30.1	3.3	47.7	10.6	48.4	90	28.3
1.0	31.6	3.4	46.9	11.5	47.6	100	26.9
1.2	35.2	3.6	46.4	12.5	46.8	110	25.8
1.4	39.3	3.8	45.8	14.5	44.6	120	24.8
1.5	40.7	4.1	45.4	16.5	42.0	140	22.8
1.6	42.1	4.3	45.4	18.5	40.2	160	21.0
1.7	43.0	4.6	45.6	20.5	39.3	180	19.7
1.8	43.2	5.1	46.9	23.0	38.9	200	18.5
1.9	42.8	5.6	48.9	25.5	38.7	220	17.6
2.0	42.5	6.1	50.0	28	38.6	250	16.3
2.2	42.5	6.6	50.4	30	38.2	300	14.4
2.4	43.3	7.1	50.8	35	37.0	350	13.0
2.6	45.1	7.6	51.1	40	35.9	400	12.2
2.8	46.8	8.1	51.0	45	34.9		
2.9	47.7	8.6	50.5	50	34.0		

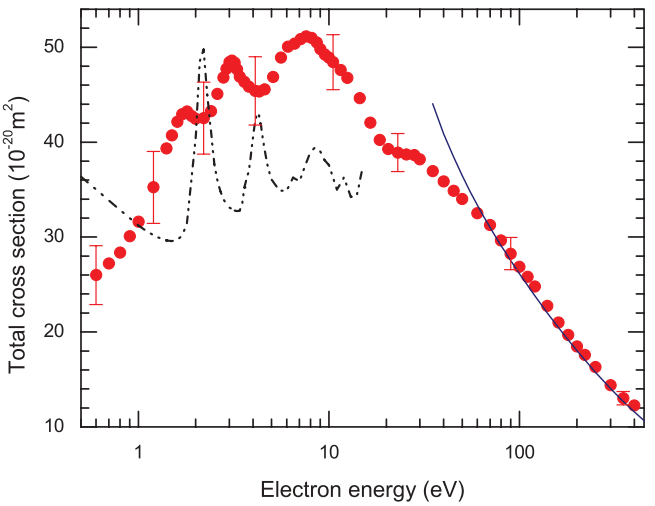

FIG. 2. (Color online) Cross sections for e-C_4H_4O scattering. Full circles are the present TCS measurements (error bars represent overall experimental uncertainties); the full line shows the present calculated (ECS + ICS) cross sections; elastic calculations of Bettega and Lima [14] in the SEP approximation are marked with the dash-dot-dot line.

trajectory (see the denominator pL in the BBL formula). For our experimental arrangement, the effect of the density drop across the orifices is partly compensated by the extension of the electron path length in the target region (cf. Ref. [24]). The systematic TCS error associated with the sample effusion is less than 2.5% for the geometry of the cell applied in the present experiment. The second serious problem is related to an imperfect discrimination by the detector system against electrons scattered into the small-angle forward direction. This *forward-scattering* effect systematically lowers the measured TCS; generally, the TCS is increasingly underestimated with the increase of the impact energy. The main contribution to this effect comes from the inability to eliminate electrons elastically scattered in the forward direction. The effect related to inelastic forward scattering is to some extent reduced by the use of the rf lens unit; in our setup, the rf analyzer enables us to discriminate electrons with a kinetic-energy difference of 0.1 eV in the case of low impact energies and about 0.5 eV at intermediates energies. We have estimated that in the present experiment, the forward-scattering effect may lower the measured low- and high-energy TCSs by about 3%–4% and by 1%–2% at intermediate energies. Other factors give systematic uncertainties which do not exceed 1% each. The overall systematic uncertainty in our measured TCS, calculated as the direct sum of potential systematic errors of measured individual quantities, amounts to about 8%–10% below 2 eV, decreases gradually to 5%–6% between 5–150 eV, and increases again up to 6%–8% at the highest energies applied.

III. CALCULATIONS

In the reported experiment the TCS for electron-furan scattering has been measured up to 400 eV only. To extend the TCS data beyond the experimental range, we have calculated intermediate- and high-energy *total* electron-scattering cross sections based on the computed integral elastic (ECS) and ionization (ICS) cross sections—then the *total* cross section is approximated with ECS + ICS. The ECS and ICS have been calculated within the independent atom (IAM) approximation [25–27] at the static-polarization level and the binary-encounter-Bethe (BEB) [28,29] method, respectively. Although, in this approach, a contribution to the total cross section of many possible processes that occur during an electron interaction with a molecule is obviously neglected, we have found that the ECS + ICS estimated this way satisfactorily reproduces the intermediate-energy experimental TCS data (e.g., Refs. [19,20,30,31]). Because the theoretical approaches applied here, as well as the computational details, have been discussed extensively earlier [32,33], only a short outline of the used methods is given in the present paper.

The integral elastic cross section for a molecule (ECS in Table II), within the IAM method, is given by the simple additivity formula:

$$\sigma(E) = \frac{4\pi}{k}\sum_{i=1}^{N} \mathrm{Im}\, f_i(\theta = 0,k) = \sum_{i=1}^{N} \sigma_i^A(E), \qquad (1)$$

where E is the energy of the incident electron, $f_i(\theta,k)$ is the scattering amplitude due to the ith atom of the molecule, θ is the scattering angle, and $k = \sqrt{2E}$ is the wave number of the incident electron. The integral elastic cross section of the ith atom of the target molecule, $\sigma_i^A(E)$, has been computed according to

$$\sigma^A = \frac{4\pi}{k^2}\left(\sum_{l=0}^{l_{\max}}(2l+1)\sin^2\delta_l + \sum_{l=l_{\max}}^{\infty}(2l+1)\sin^2\delta_l^{(B)}\right). \qquad (2)$$

Phase shifts, δ_l, have been obtained within the partial-wave analysis of the radial Schrödinger equation

$$\left(\frac{d^2}{dr^2} - \frac{l(l+1)}{r^2} - 2[V_{\mathrm{stat}}(r) + V_{\mathrm{polar}}(r)] + k^2\right) u_l(r) = 0, \qquad (3)$$

which has been solved numerically under the following boundary conditions:

$$u_l(0) = 0, \quad u_l(r) \overset{r\to\infty}{\longrightarrow} A_l \hat{j}_l(kr) - B_l \hat{n}_l(kr), \qquad (4)$$

where $\hat{j}_l(kr)$ and $\hat{n}_l(kr)$ are the Riccati-Bessel and the Riccati-Neumann functions, respectively. The electron-atom interaction has been represented by the static $V_{\mathrm{stat}}(r)$ [34] and the polarization $V_{\mathrm{polar}}(r)$ [35,36] potentials.

In the present calculations, the exact phase shifts have been calculated for l up to $l_{\max} = 50$, while those remaining, $\delta_l^{(B)}$, have been included through the Born approximation.

Within the BEB formalism, the electron-impact ionization cross section per molecular orbital is given by

$$\sigma^{\mathrm{BEB}} = \frac{S}{t+u+1}\left[\frac{\ln t}{2}\left(1 - \frac{1}{t^2}\right) + 1 - \frac{1}{t} - \frac{\ln t}{t+1}\right], \qquad (5)$$

TABLE II. Ionization (ICS) and integral elastic (ECS) cross sections calculated for electron impact on furan, C_4H_4O, molecules, in 10^{-20} m^2.

E (eV)	ICS	E (eV)	ICS	ECS	E (eV)	ICS	ECS
8.955	0	40	7.90	33.0	300	6.05	7.99
9	0.007 55	45	8.41	30.0	350	5.53	7.14
10	0.185	50	8.77	27.7	400	5.10	6.47
11	0.465	55	9.03	25.8	450	4.73	5.92
12	0.760	60	9.21	24.2	500	4.42	5.46
13	1.042	65	9.32	22.8	600	3.90	4.74
14	1.32	70	9.38	21.6	700	3.50	4.19
15	1.63	75	9.41	20.6	800	3.18	3.76
16	2.01	80	9.41	19.7	900	2.91	3.41
17	2.40	85	9.39	18.9	1000	2.69	3.13
18	2.77	90	9.35	18.2	1100	2.50	2.89
19	3.14	95	9.29	17.5	1200	2.34	2.68
20	3.49	100	9.22	16.9	1400	2.08	2.36
22.5	4.31	110	9.07	15.9	1600	1.87	2.12
25	5.07	120	8.89	15.0	1800	1.70	1.93
27.5	5.72	140	8.52	13.5	2000	1.56	1.78
30	6.29	160	8.14	12.3	2200	1.45	1.66
35	7.22	180	7.77	11.4	2500	1.30	1.54
		200	7.43	10.6	3000	1.121	1.43
		220	7.11	9.93	3500	0.985	
		250	6.67	9.09	4000	0.881	

where $u = U/B$, $t = T/B$, $S = 4\pi a_0^2 N R^2/B^2$, $a_0 = 0.5292$ Å, $R = 13.61$ eV, and T is the energy of impinging electrons. All physical quantities occurring in Eq. (5) (i.e., the electron binding energy B, the kinetic energy of the orbital U, and the orbital occupation number N), were obtained for the ground state of the furan molecule with the Hartree-Fock method using the GAUSSIAN code [37], and the GAUSSIAN 6-311G + d basis set. The valence orbital energies have been calculated with the OVGF method [38,39] implemented within the GAUSSIAN package [37].

The total cross section for electron-impact ionization (ICS in Table II) has been calculated from ionization cross sections for all molecular orbitals according to

$$\sigma^{\mathrm{Ion}} = \sum_{i=1}^{n_{\mathrm{MO}}} \sigma_i^{\mathrm{BEB}}, \tag{6}$$

where n_{MO} is the number of the given molecular orbital.

IV. RESULTS AND DISCUSSION

Our measured absolute total (TCS) and calculated elastic-plus-ionization (ECS + ICS) cross sections for e^--C_4H_4O scattering are shown in Fig. 2; numerical values of TCS are listed in Table I while values of ECS and ICS are collected in Table II, for completeness. The TCS data have been taken over the energy range from 0.6 to 400 eV. No other experimental electron-scattering TCS data or elastic and ionization cross sections are available in the literature. The ionization cross section has been calculated using the BEB method from the threshold up to 4000 eV, while the elastic cross section—in the independent atom approximation—is reported from 40 to 3000 eV. Very recent low-energy (0.5–15 eV) elastic calculations of Bettega and Lima [14] are also included in Fig. 2 for comparison.

As can be seen in Fig. 2, at the lowest applied energies, the measured TCS distinctly rises from about 26×10^{-20} m^2 at 0.6 eV up to nearly 52×10^{-20} m^2 in the TCS maximum located around 8 eV. Above 8 eV the TCS systematically decreases with the energy increase: from 8 to 20 eV the TCS function is relatively steep and falls to 39×10^{-20} m^2 at 20 eV; then the TCS becomes almost constant—between 20 and 30 eV it decreases by about 1×10^{-20} m^2 only; beyond 70 eV the TCS function decreases with increasing energy as E^{-a}, where $a \simeq 0.5$; at 400 eV the TCS falls to 12×10^{-20} m^2.

Several more or less pronounced structures are superimposed on the broad TCS enhancement between 0.6 and 20 eV. At 1.8 eV a weak and rather narrow peak appears, followed with the minimum at 2.1 eV. Around 3.1 eV a more distinct and slightly broader peak is located. The TCS structures at 1.8 and 3.1 eV correspond to two features already observed in derivatives of the transmitted electron current, first by van Veen [5] at 1.76 and 3.14 eV and more recently by Modelli and Burrow [10] at 1.73 and 3.15 eV, respectively. These features have been associated with the formation of short-lived anion states (shape resonances) created when the incoming electron is temporarily trapped into unoccupied π^* molecular orbitals. Near 1.8 eV Palmer *et al.* [7] have observed a structure in the trapped electron spectrum and attributed it to the vibrational excitation of the ground electronic state of the furan molecule via a shape resonant state. The 3.1-eV shape π^* resonance also gives a weak contribution to furanyl anion yield noticed between 3 and 4.5 eV by Muftakhov *et al.* [12] and by Sulzer *et al.* [13]. The formation of two shape resonances in this energy range has been recently confirmed in vibrationally elastic calculations by Bettega and Lima [14] and in electronically inelastic computations by da Costa *et al.* [15]. In their static-exchange plus polarization (SEP) potential approximation, the resonances are, however, shifted to slightly higher energies with respect to their location (see Fig. 2) in our TCS experiment.

Our total cross section decreases with decreasing energy in the low-energy range, 0.6–1 eV, and this may appear to contradict a simple expectation that the cross section should increase for a molecule with a permanent electric-dipole moment. In fact, Bettega and Lima [14] do calculate a slight increase in this energy range. The dipole moment of furan is quite small ($\mu = 0.66$ D; Ref. [41]), however, and we conclude that the expected increase must occur at energies below 0.6 eV, outside of our measurement range. In this connection, we point out that the cross section of CCl_2F_2, which has a similar dipole moment ($\mu = 0.51$ D), has also been observed to increase only below 0.6 eV [42].

A broad hump is visible in the TCS energy dependence above 4.5 eV. A more thorough inspection reveals that this TCS structure seems to be composed of three features: the first one is located near 6 eV, the second feature peaks close to 8 eV, and a weak shoulder is spanned between 10 and 16 eV. Although these features are barely visible in the present experiment, they may be realistic due to some support from studies concerning particular electron-scattering processes. In the excitation function of the C–H stretching vibrational modes, Motte-Tollet *et al.* [11] have observed a broad structureless peak centered around 6 eV and associated it with temporary trapping of the incoming electron in an unoccupied molecular orbital of σ^* (C–H) character. Several fragment anions have been clearly evidenced in the effective yield curves [12,13] close to 6 eV. However, they have been assumed to originate from core-excited resonances, contrary to a shape-resonance origin of the 6-eV structure suggested on the base of the vibrational excitation function [11].

The TCS feature peaked around 8 eV may also correspond to resonant processes. The formation of the core-excited resonance in the vicinity of 8.5 eV [12] results from the presence of negative fragment ions in this energy range. Elastic calculations [14] reveal a broad shape resonance near 8.5 eV.

The shoulder visible on the descending part of the TCS curve, near 14 eV, may be associated with structures visible in negative-ion spectra [12,13], observed between 9 and 13 eV, assigned to the creation of another core-excited resonance.

As can be seen in Fig. 2, the agreement between the present experiment (TCS) and calculations (ECS + ICS) is very good for energies above 70 eV; the differences do not exceed experimental uncertainties. Toward lower energies, the sum of ECS and ICS significantly overestimates the measured TCS values, because at low energies the assumptions underlying the IAM method applied for elastic calculations are not satisfied.

V. SUMMARY

In this paper we have presented the absolute total electron-scattering cross section for the C_4H_4O molecule measured in a linear transmission experiment from 0.6 to 400 eV. As the reported absolute TCSs were obtained without any normalization procedure, they can serve as one of the quantitative tests of the theoretical models and computational procedures, and for normalization of electron-scattering quantities taken in relative units.

The experimental TCS energy dependence for furan shows very distinct enhancement peaked near 8 eV with two resonant features well marked near 1.8 and 3.1 eV. Weak structures between 5 and 14 eV can be associated with core-excited resonances leading to decomposition of the temporary negative ions into the negative fragments and neutrals [12,13]. It is worth noting that the locations of these furan TCS structures on the energy scale resemble those for tetrahydrofuran (C_4H_8O) [19], although they differ in the magnitude.

We have also carried out calculations of the integral elastic (ECS) and total ionization cross (ICS) sections from intermediate up to 4-keV impact energies. Good agreement between the present computed ECS + ICS and experimental intermediate-energy TCS indicates that the approximate IAM and BEB methods adopted here look promising for the prediction of the reasonable cross sections for complex targets. The present TCS curve is also in qualitative agreement with the low-energy calculations of Bettega and Lima [14], apart from energies below 1.5 eV.

Note added in proof. Recently, the work by Khakoo *et al.* [42] was published on the combined experimental and theoretical study of the elastic low-energy electron scattering from furan. The low-energy behavior of their integral elastic cross section is in very good agreement with our total cross section data.

ACKNOWLEDGMENTS

This work has been partially supported by the Polish Ministry of Science and Higher Education (MNiSzW Project No. 2008-2009). Numerical calculations have been performed at the Academic Computer Center (TASK) in Gdańsk. The authors are grateful to Professor Marcio Bettega for providing us the numerical results of his calculations.

[1] B. Boudaïffa, P. Cloutier, D. Hunting, M. A. Huels, and L. Sanche, Science **287**, 1658 (2000).
[2] U. S. Food and Drug Administration, *Exploratory Data on Furan in Food* [http://www.fda.gov/Food/FoodSafety/FoodContaminantsAdulteration/ChemicalContaminants/Furan/default.htm]; updated Sept. 21, 2009.
[3] X. Fan and K. J. B. Sokorai, J. Food. Sci. **73**, C79 (2008); Y.-T. Liu and S.-W. Tsai, Chemosphere **79**, 54 (2010).
[4] S. Augusto, P. Pinho, C. Branquinho, M. J. Pereira, A. Soares, and F. Catarino, J. Atmos. Chem. **49**, 53 (2004); B. Cabañas, F. Villanueva, P. Martin, M. T. Baeza, S. Salgado, and E. Jiménez, Atmos. Environ. **39**, 1935 (2005).
[5] E. H. van Veen, Chem. Phys. Lett. **41**, 535 (1976).
[6] W. M. Flicker, O. A. Mosher, and A. Kuppermann, J. Chem. Phys. **64**, 1315 (1976); A. Kuppermann, W. M. Flicker, and O. A. Mosher, Chem. Rev. **79**, 77 (1979).
[7] M. H. Palmer, I. C. Walker, C. C. Ballard, and M. F. Guest, Chem. Phys. **192**, 111 (1995).
[8] A. Giuliani and M.-J. Hubin-Franskin, Int. J. Mass Spectrom. **205**, 163 (2001).
[9] D. C. Newbury, I. Ishii, and A. P. Hitchcock, Can. J. Chem. **64**, 1145 (1986).
[10] A. Modelli and P. D. Burrow, J. Phys. Chem. A **108**, 5721 (2004).
[11] F. Motte-Tollet, G. Eustatiu, and D. Roy, J. Chem. Phys. **105**, 7448 (1996).
[12] M. V. Muftakhov, N. L. Asfandiarov, and V. I. Khvostenko, J. Electron Spectrosc. Relat. Phenom. **69**, 165 (1994); V. I. Khvostenko, A. S. Vorob'yov, and O. G. Khvostenko, J. Phys. B **23**, 1975 (1990).
[13] P. Sulzer *et al.*, J. Chem. Phys. **125**, 044304 (2006).
[14] M. H. F. Bettega and M. A. P. Lima, J. Chem. Phys. **126**, 194317 (2007).
[15] R. F. da Costa, M. H. F. Bettega, and M. A. P. Lima, Phys. Rev. A **77**, 012717 (2008).
[16] M. Dampc and M. Zubek, Int. J. Mass Spectrom. **277**, 52 (2008).
[17] V. Schomaker and L. Pauling, J. Am. Chem. Soc. **61**, 1769 (1939).
[18] P. B. Liescheski and D. W. H. Rankin, J. Mol. Struct. **196**, 1 (1989).
[19] P. Możejko, E. Ptasińska-Denga, A. Domaracka, and Cz. Szmytkowski, Phys. Rev. A **74**, 012708 (2006).
[20] Cz. Szmytkowski, A. Domaracka, P. Możejko, and E. Ptasińska-Denga, J. Phys. B **41**, 065204 (2008); J. Chem. Phys. **130**, 134316 (2009).
[21] Cz. Szmytkowski, J. Phys. B **43**, 055201 (2010).
[22] M. Knudsen, Ann. Phys. (Leipzig) **31**, 205 (1910).
[23] Cz. Szmytkowski, P. Możejko, and G. Kasperski, J. Phys. B **30**, 4363 (1997); Cz. Szmytkowski and P. Możejko, Vacuum **63**, 549 (2001).
[24] R. N. Nelson and S. O. Colgate, Phys. Rev. A **8**, 3045 (1973).
[25] N. F. Mott and H. S. W. Massey, *The Theory of Atomic Collisions* (Oxford University Press, Oxford, 1965).
[26] D. Raj, Phys. Lett. A **160**, 571 (1991).
[27] K. N. Joshipura and P. M. Patel, Z. Phys. D **29**, 269 (1994).
[28] Y.-K. Kim and M. E. Rudd, Phys. Rev. A **50**, 3954 (1994).
[29] W. Hwang, Y.-K. Kim, and M. E. Rudd, J. Chem. Phys. **104**, 2956 (1996).
[30] Cz. Szmytkowski, P. Możejko, S. Kwitnewski, E. Ptasińska-Denga, and A. Domaracka, J. Phys. B **38**, 2945 (2005); Cz. Szmytkowski, P. Możejko, S. Kwitnewski, A. Domaracka, and E. Ptasińska-Denga, *ibid*. **39**, 2571 (2006).
[31] P. Możejko, A. Domaracka, E. Ptasińska-Denga, and Cz. Szmytkowski, Chem. Phys. Lett. **429**, 378 (2006).
[32] P. Możejko, B. Żywicka-Możejko, and Cz. Szmytkowski, Nucl. Instrum. Methods Phys. Res. B **196**, 245 (2002).
[33] P. Możejko and L. Sanche, Radiat. Environ. Biophys. **42**, 201 (2003).
[34] F. Salvat, J. D. Martinez, R. Mayol, and J. Parellada, Phys. Rev. A **36**, 467 (1987).
[35] N. T. Padial and D. W. Norcross, Phys. Rev. A **29**, 1742 (1984).

[36] X. Zhang, J. Sun, and Y. Liu, J. Phys. B **25**, 1893 (1992).
[37] M. J. Frisch *et al.*, GAUSSIAN 03, Revision B.05 (Gaussian, Pittsburgh, 2003).
[38] J. V. Ortiz, J. Chem. Phys. **89**, 6348 (1988).
[39] V. G. Zakrzewski and W. von Niessen, J. Comput. Chem. **14**, 13 (1994).
[40] *Handbook of Chemistry and Physics*, 76th ed., edited by D. R. Lide (Chemical Rubber, Boca Raton, 1995–1996).
[41] L. G. Christophorou and J. K. Olthoff, *Fundamental Electron Interactions with Plasma Processing Gases* (Kluwer/Plenum, New York, 2004); see Fig. 6.40.
[42] M. A. Khakoo, J. Muse, K. Ralphs, R. F. da Costa, M. H. F. Bettega, and M. A. P. Lima, Phys. Rev. A **81**, 062716 (2010).